Genome-wide identification of functional tRNA-derived fragments in Senescence-accelerated mouse prone 8 brain

Shuai Zhang[1-2#], Hejian Li[1-2], Ling Zheng[1-2], Hong Li[1-2], Chengqiang Feng[1-2] Wensheng Zhang[1-3*]

[1]Beijing Key Laboratory of Traditional Chinese Medicine Protection and Utilization, Faculty of Geographical Science, Beijing Normal University, Beijing 100875, China; [2]Engineering Research Center of Natural Medicine, Ministry of Education, Faculty of Geographical Science, Beijing Normal University, Beijing 100875, China; [3]National and Local United Engineering Research Center for Panax Notoginseng Resources Protection and Utilization Technology, Kunming 650000, China.

* To whom correspondence should be addressed. Tel: +86 010 62200669; Fax: +86 010 62200669; Email: zwslabpaper@sina.com

[#]was the first author of the paper

Address for correspondence: C Building, Beijing Normal University Science Park, No. 12, Xueyuan Southern Street, Haidian District, Beijing, P.R. China, 100088.

Abstract

tRNA-derived fragments (tRFs) have been linked previously to the development of various diseases, such as cancer, viral infectious disease, Parkinson's disease, and intellectual disability. However, the link between tRFs and Alzheimer's disease (AD) has not been understood. RNA sequencing, a state-of-the-art technology, has largely increased the level of research on tRFs in AD. In this study, we investigated the changes in tRFs in SAMP8 and SAMR1 mouse brains at 7 months of age. A total of 596 tRF transcripts were discovered. Among these transcripts, 13, including 4 upregulated and 9 downregulated transcripts, were found to be differentially expressed in the SAMP8 mice. Then, we obtained 137 potential target genes through an miRNA-like pathway. Gene Ontology (GO) survey indicated that these target genes are implicated in AD pathogenesis from different aspects, for example, postsynaptic density (GO: 0014069). Furthermore, the tRFs that most likely affect the progression of AD by miRNA-like pattern were estimated and displayed in detail, such as AS-tDR-011775 acted on Mobp immediately and Camk2n1 was targeted by AS-tDR-011389. Actually, the tRFs participated in the regulation of gene expression by means other than the miRNA-like pattern. Therefore, these 13 dysregulated tRFs may hold consequences far into the future and can be attractive biomarkers and valid targets. In brief, our study is the first to provide a comprehensive analysis on tRFs in SAMP8 mouse brain, and this breakthrough identified promising new targets for the therapeutic intervention of AD.

Keywords: AD; tRFs; SAMP8; genome-wide; RNA sequencing; miRNA-like

Author summary

Alzheimer's disease (AD) is one of the most common amnesic disorder. The pathogenesis of AD is complex and contributed by both genetic and environmental factors. Recent studies reveal a potential link between tRNA-derived fragments (tRFs) and neurodegenerative diseases. However, there is no evidence of a correlation between AD and tRFs. In this study, we describe a mouse model of AD, called senescence-accelerated mouse prone 8 (SAMP8), which has an age-related spontaneous deterioration in learning and memory abilities. Furthermore, RNA sequencing, an up-to-date technology, is used. In these cases, we systematically discuss the possible implication of tRFs in AD. The selected tRFs are considered strong future candidates to combat this life-threatening disease. This finding provides a novel molecular strategy to profoundly affect diagnosis and therapy in the future.

Introduction

Alzheimer's disease (AD) is a progressive neurodegenerative disorder [1]. Alois Alzheimer, a German physician, first described AD in 1906 [2]. Its clinical symptoms are characterized by age-dependent memory loss, personality change, impairments of multiple cognitive functions, and behavioral deficit [3-5]. This disease brings great agony and inconvenience to the patient's life. Some countries, such as China, Japan, and Italy, have become aging societies that have considered the problem on the prevention and cure of AD a public concern. Although many theories, including Aβ deposition, tau phosphorylation, synapse injury, mitochondrial dysfunction, neuron loss, oxidative stress, insulin resistance, gene mutation, and inflammatory dysfunction, have attempted to explain the origin of AD [6-9], few treatment options are available to prevent or reverse this condition. The phrase "DNA-mRNA-protein-cell-tissue-organ-individual-population" actually referred to the flow of genetic information. This notion indicates that gene expression and regulation play an important role in the occurrence and development of the disease. Currently, gene expression regulation and AD have drawn increasing attention among researchers.

In a previous work, we analyzed the changes of lncRNA, circRNA, miRNA, and DNA methylation in the brain of senescence-accelerated mouse prone 8 (SAMP8), and the related mechanisms of gene expression regulation in AD [10-12]. As high-throughput sequencing technology advances, a novel class of small non-coding RNAs (ncRNAs) derived from tRNAs was detected and called tRNA-derived fragments (tRFs), with lengths ranging from 14-36 nucleotides (nt) [13, 14]. They can be classified into tRF-5, tRF-3, tRF-1, i-tRF, and tiRNA (tiRNA-3 and tiRNA-5) [15-17]. Recently, many studies have shown that tRFs are implicated in mediating complex pathological processes of diverse illnesses, such as cancer and viral infectious disease [18, 19]. More importantly, tRFs play a major role in stabilizing the nervous system by helping regulate amyotrophic lateral sclerosis (ALS) and Parkinson's disease (PD) [20, 21]. tRFs and neurodegeneration are certainly closely related. Thus, whether tRFs can affect the progression of AD remains to be investigated. The role of tRFs in AD is poorly understood, at least, to date. Clearly this aspect is a valuable research direction.

Given these findings and requirements, we characterized the expression of tRFs in the brain of SAMP8 and senescence-accelerated mouse resistant 1 (SAMR1) mice at 7 months of age through deep RNA sequencing (tRFs-seq) in this study. The alterations of brain structure and function in SAMP8 mice display high similarity to AD patients [22]. Hence, the SAMP8 mouse is a desirable AD model. The SAMR1 strain undergoes a normal aging process and is often used as the reference group [23]. Our study is the first to provide systematic insight into the profiling of the tRF transcriptome in the AD model SAMP8 mouse. These tRFs may be potential therapeutic targets and diagnostic markers in AD.

Results

Memory impairments at the 7-month stage in the SAMP8 mice

MWM test was used to perform training and probe trials to evaluate the learning and memory deficits in 7-month-old SAMP8 mice. The result for the hidden platform test is shown in **Fig 1A**; the SAMP8 mice entailed a longer time to find the platform than that of the SAMR1 mice ($p < 0.05$). The spatial probe test was performed next. **Fig 1B** clearly illustrates that the SAMR1 mice searched for the destination location purposefully, whereas the SAMP8 mice swam aimlessly in the pool. The number of times the platform was traversed and the time percentage at the target quadrant were significantly lower in the SAMP8 group than in the SAMR1 group ($p < 0.05$, **Figs 1C and 1D**). The SAMP8 mice also performed normally in swimming speed ($p > 0.05$, **Fig 1E**); this result suggests the lack of motor and visual dysfunction in the SAMP8 mice. Evidently, the 7-month-old SAMP8 mice presented impaired memory and poor learning skills, which were consistent with AD clinical symptoms.

tRFs sequencing roundup

A total of 69,772,438 raw reads (34,909,558 for the SAMP8 mice and 34,862,880 for SAMR1 mice) were generated. After the 5′- and 3′-adaptors were trimmed, low-quality reads were removed, and ≤16 bp reads were filtered, a total of 68,118,335 clean reads (33,886,463 for SAMP8 mice and 34,231,872 for SAMR1 mice) were found in the two groups. Most clean reads were 22, 21, 23, and 45 nt in length for both groups (**S1A and S1B Figs**). Then, the high-quality clean data were mapped to the mouse mature-tRNA and pre-tRNA sequences from GtRNAdb by NovoAlign software (v2.07.11). In accordance with the comparison results, 596 tRFs were detected. Interesting, some tRFs were generated from the primary tRNA transcripts but not the 3′ ends; these tRFs may comprise a new type of tRF (designated herein as novel tRF). These 596 tRFs (570 conventional tRFs and 26 novel tRFs) were used for subsequent analysis.

Dysregulation of several tRFs in the SAMP8 mouse brain

To investigate whether tRF production was dysregulated in the SAMP8 mouse brains, we used transcripts per million (TPM) to estimate the expression level of the tRF transcripts. The expressed level of each conventional subtype showed a similar proportion between the two groups. The percentages were approximately 45% tRF-5,

26% tiRNA (2% tiRNA-3 and 24% tiRNA-5), 19% i-tRF, 5% tRF-3, and 5% tRF-1 (**Figs 2A and 2B**). Novel tRF showed a similar expression level with that of tiRNA-3. As a result, 13 significantly differentially expressed tRFs were identified, namely, 4 upregulated and 9 downregulated tRFs in SAMP8 mice ($p < 0.01$ and fold changes ≥ 2, **S1 Table)**. Cluster analysis of the differentially expressed tRFs was conducted with a heat map (**Fig 3**). In the SAMP8 group, three samples were clustered together. The same situation occurred in the SAMR1 group.

Quantitative confirmation

qPCR technique was performed to confirm the differential expression identified in our tRF-seq experiment. We randomly selected four dysregulated tRFs, including two upregulated and two downregulated tRFs, in the SAMP8 mice relative to those of the SAMR1 mice. As shown in **Fig 4**, all the selected tRF transcripts were detected and exhibited differences between the two groups. Collectively, the qPCR results corresponded highly with the tRF-seq data.

Target gene

We proposed that the tRFs played extremely important roles in the regulation of gene expression. These tRFs may be involved in controlling gene transcription and translation in various means. Among these pathways, a highly important patterns is the miRNA-like behavior of tRFs. On the basis of this concept, we pioneered the identification of tRF–mRNA pairs in the SAMP8 brain through our mRNA-seq and tRFs-seq data. We chose to use 482 mRNAs and 13 tRFs that were differentially expressed in this study. The results are presented in **S2 Table**; 137 potential target genes were identified.

GO enrichment

GO investigation was performed on the above-mentioned target genes. The results revealed that 17 GO terms were significantly enriched ($p < 0.05$, **S3 Table**). Importantly, several AD-associated terms were detected, including negative regulation of the canonical Wnt signaling pathway (GO: 0090090), postsynaptic density (GO: 0014069), and dendrite (GO: 0030425). Overall, these protein-coding genes may be regulated by tRFs through an miRNA-like pathway involved in AD.

Relevance research

To obtain an improved understanding of the relationship between tRFs and AD, we set three restrictions. For the first factor, the tRFs and their target genes must be expressed differently between the SAMP8 and SAMR1 mice. For the second factor, the trend of expression of tRF and its target gene should be the opposite in the brain. These trends include two cases: one case corresponds to the tRF (upregulated in the SAMP8 mice)-mRNA (downregulated in the SAMP8 mice), and the other case refers to the tRF (downregulated in the SAMP8 mice)-mRNA (upregulated in the SAMP8 mice). For the last requirement, the selected pairs (tRF-mRNA) should possess a close relationship with pathologic process of AD. If a pair meets the above criteria, the pair can be selected.

Some examples are as follows. Camk2n1, an endogenous CaMKII inhibitor protein, showed a direct effect on synaptic CaMKII-NMDAR binding and played an important role in LTP regulation [24]. We found that the expression of Camk2n1 in the SAMP8 mouse brain was significantly higher than that in the SAMR1 mice. AS-tDR-011389 presented the low expression level in the SAMP8 mouse brain and can target Camk2n1; AS-tDR-011775 acted on Mobp immediately. Mobp may play a role in controlling axonal diameter and in keeping axons round [25]. More specific details were listed in **Table 1**. We predicted that these tRFs most likely participate in the genesis and development of AD.

Herein, we reiterate that besides the miRNA-like pattern, tRFs can also exert regulatory functions in other manners. For example, tRFs displaced the eIF4G translation initiation factor from mRNAs and participated in post-transcriptional regulation [26]. The tRFs were capable of competing for the mRNA binding sites of YBX1 to suppress cancer progression [27]. Therefore, the functions of these tRFs (13 significant differentially expressed tRFs) may hold important meanings for the control and prevention of AD.

Discussion

In year 2009, Cole *et al*. first identified tRFs from cultured HeLa cells [28]. Then, tRFs were detected in other kinds of human cells or tissues [17, 18, 29]. tRFs were also evaluated in plants or other animals, such as barley [30] and cattle [31]. Given their widespread presence, the tRFs are expected to play key roles in many physiological and pathological processes. Two systematic reviews showed that the expression of tRFs was altered in a range of diseases and suggest a close relationship between tRFs and diseases [32, 33]. More significantly, the anomalies of tRFs exerted a great influence on neurodegeneration and related diseases [17, 20, 21]. With aging, tRFs undergo dynamic changes in the mammalian brain [34]. AD is the most common neurodegenerative disorder worldwide and the leading cause of dementia among older adults [1-5]. This disease is highly complex and only confirmed by brain examination after death. No valid therapeutic options are available to prevent or reverse this disease. Finding early diagnostic biomarkers and novel therapeutic targets is thus imperative. Recent studies have shifted focus to dysregulated gene alterations and regulations in AD. We have conducted considerable work previously on this aspect, including on lncRNA, miRNA, circRNA, and DNA methylation [10-12]. As a special and relative new ncRNA, tRFs may be correlated with AD development and advance by regulating the expression of specific genes. However, no report exists on the relationship between tRFs and AD. In the present study, the primary goal is to identify AD-associated tRFs as much as possible. Unfortunately, the human tissue samples are very difficult to collect for several reasons. Given this data, we selected an idealized animal AD model to break past the limit. Kang *et al*. demonstrated that the 7-month-old SAMP8 mouse can be considered a valid animal model of AD [35]. Our MWM test also confirmed that the SAMP8 mice exhibited memory impairments and learning deficits at such age; these signs were the core clinical features observed in AD patients. Moreover, high-throughput sequencing (RNA-seq) was applied in our study and allowed the

identification of potential AD-associated tRFs in unprecedented detail. On the basis of the results, the candidate tRFs can be explored as novel sensitive factors for AD control and prevention in the future.

First, we discovered 596 tRF transcripts in SAMP8 and SAMR1 mouse brains at 7 months of age. On the basis of the standard classification [15], these tRFs were classified into various subtypes, including 69 tiRNA-5, 14 tiRNA-3, 94 tRF-3, 94 tRF-5, 78 tRF-1, 232 i-tRF, and 26 novel tRF. The novel tRFs are those tRFs derived from the primary tRNA transcript but not the 3′ end, which result in a new type of tRF. AS-tDR-001441, AS-tDR-000581, AS-tDR-005305, AS-tDR-007364, and so on belong to the novel tRFs. Interestingly, 11 transcripts were part of the tRF-1 as well as part of other subtypes; for example, AS-tDR-009308 was both tRF-1 and tRF-3. In summary, the majority of tRFs (tiRNA-5, tiRNA-3, tRF-3, tRF-5, and i-tRF) identified in our samples originated from mature tRNAs, whereas the tRFs (i-tRF and novel tRF) generated from the primary tRNAs were in the minority. This phenomenon is consistent with previous reports [31, 36, 37].

Second, we calculated the expression of each tRF transcript through TPM. Although i-tRF was the subtype with the most tRF transcripts, the expression levels of the i-tRF transcripts were not the highest. The tRF-5 subtype achieved the highest expression levels. On the opposite end, the expression levels of the tiRNA-3 and novel tRF subtype were the lowest. The 5′-derived tRFs (tRF-5 and tiRNA-5) were the most abundant class of tRFs between the two groups, followed by i-tRF, with the 3′-derived tRFs (tiRNA-3, tRF-3 and tRF-1) and novel tRF least.

Third, the tRFs with fold changes ≥ 2 and $p < 0.05$ were selected as the significantly differentially expressed tRFs. A total of 13 dysregulated tRFs were detected, including 4 upregulated and 9 downregulated tRFs in the SAMP8 mice relative to those of the SAMR1 mice. Briefly, AS-tDR-011775, AS-tDR-011438, AS-tDR-006835 and AS-tDR-005058 expressed significantly higher in SAMP8 mice brain than that in SAMR1 mice brain. By contrast, AS-tDR-013428, AS-tDR-011389, AS-tDR-009392, AS-tDR-012690, AS-tDR-010654, AS-tDR-008616, AS-tDR-010789, AS-tDR-011670 and AS-tDR-007919 expression were significantly higher in SAMR1 mice brain. Through cluster analysis, we hypothesized the relationships among samples. In our study, the result of cluster analysis showed a distinguishable tRF expression profiling between the two groups. We were aware that tRFs are tied closely to various diseases [32, 33]. It is speculated that these dysregulated tRFs can play functional roles in AD pathogenesis. These tRFs may at least serve as potential biomarkers to detect AD early.

Fourth, tRFs are proven to play key roles in the process of gene expression and regulation in several manners. A fundamental path is to behave similar to miRNAs [38, 39]. Given previous experience, the interactions of the protein-coding genes and lncRNAs were determined through miRanda, TargetScan, and Perl script. We then identified 137 potential genes. Through GO survey, these target genes were found to be

involved in AD pathogenesis from different aspects, such as dendrite (GO: 0030425), postsynaptic density (GO: 0014069), and negative regulation of the canonical Wnt signaling pathway (GO: 0090090). Furthermore, several special filter conditions were set to select the most likely tRF–mRNA pairs involved in the regulation of AD progression under an miRNA-like pattern. We mentioned the AS-tDR-011389-Camk2n pair, and AS-tDR-011775- Mobp pair in previous texts [24, 25]. Rpsa, a gene found to facilitate the production and internalization of neurotoxic Aβ peptide [40], was targeted by AS-tDR-010654 and AS-tDR-013428. AS-tDR-006835 can act on Dio2, which is a risk factor for AD [41]. Li *et al*. revealed that Tac1 was significantly downregulated in the whole brain, frontal lobe, temporal lobe, and hippocampus [42]. Tac1 was controlled by AS-tDR-011438. The other additional altered pairs identified in our study are listed in Table 1. Interestingly, one AD-associated gene may be targeted by several tRFs. For instance, Park2 [43] was regulated by AS-tDR-011438 and AS-tDR-011775. In another aspect, one tRF can dominate an increased number of AD-associated genes. AS-tDR-011389 is a good example and controlled P2ry1 [44] and Camk2n1 [24]. This observation suggests that the miRNA-like mechanism of tRFs in the regulation of gene expression is complex in AD. Moreover, the participation of tRFs in gene expression regulation by other means must be emphasized. tRFs are capable of displacing the eIF4G translation initiation factor from mRNAs [26]. tRFs suppress breast cancer progression via YBX1 displacement [27]. These tRFs (13 dysregulated tRFs) may hold important implications in the control and prevention of AD. Therefore, our ongoing effort will focus on the functions of these high-potential tRFs in AD at the molecular level. This goal is expected to be a massive challenge for many years to come.

We also used qPCR to detect the accuracy and reliability of tRF-seq in our study. Four dysregulated tRF transcripts were chosen randomly and used for measurement. As a result, all of the selected tRF transcripts were recognized and showed differential expression between the SAMP8 and SAMR1 brains at 7 months of age. This finding demonstrated that our pipeline was highly strict in identifying putative tRFs and laid a solid foundation for further exploration and experimentation.

Conclusion

Our study investigated tRF profiles in the brain of SAMP8 and SAMR1 mice at 7 months' age and offered a lead for the further investigation of the biological role and marker potential of novel tRFs in AD. The study of tRFs in AD has merely commenced but will certainly open a new frontier in the development of new therapeutic targets for AD in the future.

Materials & methods

Preparation of animals

In this study task, we purchased SAMP8 mice (n = 15, 3 months of age, male, pathogen and virus free) and SAMR1 mice (n = 15, 3 months of age, male, pathogen and virus free) from Beijing WTLH Biotechnology Co., Ltd. Then, the mice were maintained in

separate cages with standard conditions and allowed to obtain food and water freely until 7 months old. Eight animals of each group were chosen at random for the Morris water maze (MWM). The remaining mice were given general anesthesia, sacrificed by cervical dislocation, and dissected to obtain their cerebral cortices. The tissues were immediately preserved in liquid nitrogen at -196 ℃ for tRF sequencing and other experiments.

All experimentation on the mice complied with the "Guide for the care and use of laboratory animals" [45] and were permitted by the Institutional Animal Care and Use Committee of Beijing Normal University.

Behavioral studies

The spatial learning and memory of SAMP8 mice at the 7-month-old stage were evaluated through the MWM as previously described [46]. Briefly, the mice were familiarized with the MWM environment on the day before the program. In the hidden platform experiment (days 1-5), we set a platform in a suppositive quadrant. The mice were trained twice a day for 5 days. The mice were then allowed to swim for 90 s during each training. The escape latency was recorded through a special software once they touched the platform. However, if a mouse failed to reach the platform within the stipulated time, we helped find the platform, and the escape latency was regarded as 90 s. In the spatial probe experiment (day 6), we withdrew the platform and allowed the mice to swim freely for 1 min. The time spent in the target quadrant, the number of platform crossing, and the swimming trajectory of each mouse within 1 min were recorded. Finally, all experiments were performed simultaneously every day, and the investigator was unaware of the mouse genotypes throughout the trial.

Library preparation

Six cDNA libraries were constructed, i.e., three for the SAMP8 mice and three for the SAMR1 mice. Agarose gel electrophoresis (AGE) was adopted to examine the integrality of total RNA samples and were quantified on the NanoDrop ND-2000 instrument. Total RNA samples were first pretreated as follows to remove some RNA modifications that interfere with small RNA-seq library construction: 3′-aminoacyl deacylation to 3′-OH for 3′ adaptor ligation, 3′-cP removal to 3′-OH for 3′ adaptor ligation, 5′-OH phosphorylation to 5′-P for 5′-adaptor ligation, m1A and m3C demethylation for efficient reverse transcription. These steps were conducted to prepare a gene library: 1) 3′-adapter ligation, 2) 5′-adapter ligation, 3) cDNA synthesis, 4) PCR amplification, and 5) size selection of ~135-160 bp PCR-amplified fragments (corresponding to ~15-40 nt small RNAs). The Agilent bioanalyzer 2100 system was used to assess library quality. Finally, the libraries were pooled in equal amounts depending on the quantification results.

Sequencing

The libraries were denatured and diluted to a loading volume of 1.3 ml and loading concentration of 1.8 pM with 0.1 M NaOH. The diluted libraries were then loaded onto

a reagent cartridge and forwarded to a sequencing run on the Illumina NextSeq 500 system by using a NextSeq 500/550 V2 kit (Illumina) in accordance with manufacturer's instructions. Sequencing was carried out in 50 cycles.

Quality control and mapping summary

Raw data files in FASTQ format were generated through Illumina NextSeq 500. The sequencing quality was shown by quality score. This quality score was then represented by Q, which is the −10×log10 transformed probability of the base calling being incorrect. Q30 means the incorrect probability is 0.001. If the number is larger than 30, the incorrect probability is less than 0.001, i.e., > 99.9% correct. Generally, when most of the quality scores are above 30, the sequence is of high quality.After Illumina quality control, the sequencing reads were 5′,3′-adaptor trimmed, filtered for ≥ 16 nt by the Cutadapt software [47], and aligned to mature-tRNA and pre-tRNA sequences from GtRNAdb [48] by using the NovoAlign software (v2.07.11) [49].

Expression analysis

tRF expression levels were measured and normalized as read counts per million of total aligned tRF reads (TPM) [50]. tRFs with fold changes ≥ 2 and p value < 0.01 were selected as the significantly differentially expressed tRFs between SAMP8 and SAMR1.

Quantitative real-time PCR

The results of tRFs-seq were validated through qPCR. Among the significantly dysregulated tRF transcripts, four were randomly selected. qPCR was performed with the ViiA7 Real-time PCR System, rtStar™ tRF&tiRNA Pretreatment Kit (Arraystar), rtStar™ First-Strand cDNA Synthesis Kit (Arraystar), and 2× PCR master mix (Arraystar). The specific quantitative primers for the four transcripts are listed in **S4 Table**. The 10 μL reaction volume contained 0.5 μL of each primer, 2 μL of H_2O, 2 μL of cDNA, and 5 μL of 2× Master Mix. The conditions were 95 ℃ for 10 min followed by 40 cycles (95 ℃ for 10 s and 60 ℃ for 60 s). Each experiment was performed in triplicate.

Target prediction

Research has shown that a highly important function of tRFs is to behave like miRNAs and repress the expression of endogenous targets [38, 39]. In other words, the tRFs pair with the 3′UTRs of the mRNAs to direct the latter's post-transcriptional repression. Given this observation, we used miRanda, TargetScan, and Perl script to systematically predict the tRF–mRNA interaction. In this research, the expression levels of the tRFs and mRNAs showed significant difference between the SAMP8 and SAMR1 mice and were hence analyzed. Our previous study [10] revealed that 482 mRNA transcripts were differentially expressed between SAMP8 and SAMR1 mouse brains at 7 months of age (adjusted p value < 0.05, **S5 Table**).

Gene Ontology (GO) survey

GO enrichment analysis was applied to the target genes of tRFs. GOseq R package was

then used to perform GO analysis [51]. GO terms with p value < 0.05 were recognized as significant enrichment.

Statistical analysis

The test results were analyzed by SPSS 20.0 software. All data were presented as the mean ± standard error of the mean (SEM). $p < 0.05$ represented significant difference. The difference of the escape latency data in the MWM test was compared with two-way ANOVA. Student's t test was applied to compare the qPCR results, and the remaining data of the MWM test.

Figure legends

Fig 1. Memory impairments in SAMP8 mice. MWM test was used to evaluate the learning and memory deficits in 7-month-old SAMP8 and SAMR1 mice (n = 8/group). (A) Escape latencies in the hidden platform experiment. (B) Swimming paths during the spatial probe experiment. (C) Number of crossings during the probe trial. (D) Time spent in the target quadrant in the probe trial test. (E) The swimming speeds of the mice were similar between the two groups. *$p < 0.05$.

Fig 2. Proportions of tRF-5, tiRNA, i-tRF, tRF-3, and tRF-1 in the two groups. (A) Proportions in the SAMP8 mice. (B) Proportions in the SAMR1 mice.

Fig 3. Cluster analysis of differentially expressed tRFs through a heat map. Red indicates an increased expression, and blue indicates a decreased expression.

Fig 4. Validation of dysregulated tRFs by qPCR between SAMP8 and SAMR1 mice. The U6 gene was used as a housekeeping internal control. The relative expression of each tRF was represented as mean ± SEM (n = 3). *Significant difference at $p < 0.05$.

Table

Table 1. tRFs are most possibly involved in AD pathogenesis through an miRNA-like pattern

tRFs	SAMP8_TPM	SAMR1_TPM	*P* value	Potential target gene
AS-tDR-005058	224.88	0.00	0.004333786	Erc1 (SAMP8↓)
AS-tDR-006835	179.04	0.00	0.000780738	Dio2 (SAMP8↓)
AS-tDR-011775	162.75	0.00	5.6518E-05	Mobp, Park2 (SAMP8↓)
AS-tDR-011438	167.05	0.00	0.000660958	Park2, Tac1, Tubb4a, Lamc3 (SAMP8↓)
AS-tDR-011389	0.00	176.24	0.00103563	P2ry1, Camk2n1 (SAMP8↑)
AS-tDR-010654	0.00	269.77	0.002943975	Rpsa (SAMP8↑)
AS-tDR-013428	0.00	192.05	2.25358E-05	Rpsa (SAMP8↑)

Note: SAMP8↓ means the gene that is downregulated in SAMP8 mice brain; SAMP8↑means the gene that is upregulated in SAMP8 mice brain

Supporting information

S1 Fig. Sequence length distribution of clean reads in the two groups. (A) Sequence length distribution in the SAMP8 mice. (B) Sequence length distribution in the SAMR1 mice.

S1 Table. Significantly and differentially expressed tRF transcripts between SAMP8 and SAMR1 mice.

S2 Table. Potential targets of tRFs: tRF–mRNA pairs.

S3 Table. GO enrichment analysis of the tRF-targeting genes.

S4 Table. Primers used in qPCR analysis.

S5 Table. Significantly and differentially expressed mRNA transcripts between SAMP8 and SAMR1 mice.

Acknowledgements

We thank all contributors to this study. We also thank Mr Hui Ma and his colleagues at KangChen Bio-tech for their assistance.

Funding

This work was supported by the National Nature Science Foundation of China (81771152), the National Key Research and Development Program of China (SQ2017YFC170021-05), and the Beijing Joint Project for the Central-Affiliated University (2017-01).

Authors' contributions

SZ WZ conceived and designed the experiments. SZ HL LZ HL performed the experiments. SZ HL CF analyzed the data. SZ WZ contributed to the acquisition of reagents/materials/analysis tools. SZ wrote the paper.

Competing interests

We declare that there are no competing financial interests in relation to the work described.

References

1. Yang X, Tohda C. Heat shock cognate 70 inhibitor, VER-155008, reduces memory deficits and axonal degeneration in a mouse model of Alzheimer's Disease. Front Pharmacol. 2018; 9: 48.

2. Dahm R. Alzheimer's discovery. Curr Biol. 2006; 16(21): R906-R910.
3. Jahn H. Memory loss in Alzheimer's disease. Dialogues Clin Neurosci. 2013; 15(4): 445-454.
4. Weintraub S, Wicklund AH, Salmon DP. The neuropsychological profile of Alzheimer disease. Cold Spring Harb Perspect Med. 2012; 2(4): a006171.
5. Balsis S, Carpenter BD, Storandt M. Personality change precedes clinical diagnosis of dementia of the Alzheimer type. J Gerontol B Psychol Sci Soc Sci. 2005; 60(2): P98-P101.
6. Swerdlow RH. Pathogenesis of Alzheimer's disease. Clin Interv Aging. 2007; 2(3): 347-359.
7. Alavi Naini SM, Soussi-Yanicostas N. Tau hyperphosphorylation and oxidative stress, a critical vicious circle in neurodegenerative tauopathies? Oxid Med Cell Longev. 2015; 2015: 151979.
8. Mattson MP. Pathways towards and away from Alzheimer's disease. Nature. 2004; 430(7000): 631-639.
9. Ferreira ST, Clarke JR, Bomfim TR, De Felice FG. Inflammation, defective insulin signaling, and neuronal dysfunction in Alzheimer's disease. Alzheimers Dement. 2014; 10(1): S76-S83.
10. Zhang S, Qin CX, Cao GQ, Xin WF, Feng CQ, Zhang WS. Systematic analysis of long noncoding RNAs in the senescence-accelerated mouse prone 8 brain using RNA sequencing. Mol Ther Nucleic Acids. 2016; 5(8): e343.
11. Zhang S, Zhu DN, Li H, Li HJ, Feng CQ, Zhang WS. Characterization of circRNA-associated-ceRNA networks in a senescence-accelerated mouse prone 8 brain. Mol Ther. 2017; 25(9): 2053-2061.
12. Zhang S, Qin CX, Cao GQ, Guo LM, Feng CQ, Zhang WS. Genome-wide analysis of DNA methylation profiles in a senescence-accelerated mouse prone 8 brain using whole-genome bisulfite sequencing. Bioinformatics. 2017; 33(11): 1591-1595.
13. Kumar P, Kuscu C, Dutta A. Biogenesis and function of transfer RNA-related fragments (tRFs). Trends Biochem Sci. 2016; 41(8): 679-689.
14. Keam SP, Hutvagner G. tRNA-derived fragments (tRFs): emerging new roles for an ancient RNA in the regulation of gene expression. Life. 2015; 5(4): 1638-1651.
15. Lee YS, Shibata Y, Malhotra A, Dutta A. A novel class of small RNAs: tRNA-derived RNA fragments (tRFs). Genes Dev. 2009; 23: 2639-2649.
16. Li S, Hu GF. Emerging role of angiogenin in stress response and cell survival under adverse conditions. J Cell Physiol. 2012; 227: 2822-2826.
17. Schaffer AE, Eggens VRC, Caglayan AO, Reuter MS, Scott E, Coufal NG, et al. CLP1 founder mutation links tRNA splicing and maturation to cerebellar development and neurodegeneration. Cell. 2014; 157(3): 651-663.
18. Zhou K, Diebel KW, Holy J, Skildum A, Odean E, Hicks DA, et al. A tRNA fragment, tRF5-Glu, regulates BCAR3 expression and proliferation in ovarian cancer cells. Oncotarget. 2017; 8(56): 95377-95391.
19. Yeung ML, Bennasser Y, Watashi K, Le SY, Houzet L, Jeang KT. Pyrosequencing of small non-coding RNAs in HIV-1 infected cells: evidence for the processing of a viral-cellular double-stranded RNA hybrid. Nucleic Acids Res. 2009; 37(19): 6575-

6586.
20. Ivanov P, O'Day E, Emara MM, Wagner G, Lieberman J, Anderson P. G-quadruplex structures contribute to the neuroprotective effects of angiogenin-induced tRNA fragments. Proc Natl Acad Sci U S A. 2014; 111(51): 18201-18206.
21. Van Es MA, Schelhaas HJ, Van Vught PWJ, Ticozzi N, Andersen PM, Groen EJ, et al. Angiogenin variants in Parkinson disease and amyotrophic lateral sclerosis. Ann Neurol. 2011; 70(6): 964-973.
22. Butterfield DA, Poon HF. The senescence-accelerated prone mouse (SAMP8): a model of age-related cognitive decline with relevance to alterations of the gene expression and protein abnormalities in Alzheimer's disease. Exp Gerontol. 2005; 40(10): 774-783.
23. Zhang GR, Cheng XR, Zhou WX, Zhang YX. Age-related expression of STUB1 in senescence-accelerated mice and its response to anti-Alzheimer's disease traditional Chinese medicine. Neurosci Lett. 2008; 438(3): 371-375.
24. Gouet C, Aburto B, Vergara C, Sanhueza M. On the mechanism of synaptic depression induced by CaMKIIN, an endogenous inhibitor of CaMKII. PLoS One. 2012; 7(11): e49293.
25. Sadahiro S, Yoshikawa H, Yagi N, Yamamoto Y, Yanagihara T, Kimura M, et al. Morphometric analysis of the myelin-associated oligodendrocytic basic protein-deficient mouse reveals a possible role for myelin-associated oligodendrocytic basic protein in regulating axonal diameter. Neuroscience. 2000; 98(2): 361-367.
26. Ivanov P, Emara MM, Villen J, Gygi SP, Anderson P. Angiogenin-induced tRNA fragments inhibit translation initiation. Mol Cell. 2011; 43: 613-623.
27. Goodarzi H, Liu X, Nguyen HCB, Zhang S, Fish L, Tavazoie SF. Endogenous tRNA-derived fragments suppress breast cancer progression via YBX1 displacement. Cell. 2015; 161(4): 790-802.
28. Cole C, Sobala A, Lu C, Thatcher SR, Bowman A, Brown JW, et al. Filtering of deep sequencing data reveals the existence of abundant Dicer-dependent small RNAs derived from tRNAs. RNA. 2009; 15: 2147-2160.
29. Wang Q, Lee I, Ren J, Ajay SS, Lee YS, Bao X. Identification and functional characterization of tRNA-derived RNA fragments (tRFs) in respiratory syncytial virus infection. Mol Ther. 2013; 21: 368-379.
30. Hackenberg M, Huang PJ, Huang CY, Shi BJ, Gustafson P, Langridge P. A comprehensive expression profile of microRNAs and other classes of non-coding small RNAs in Barley under phosphorous-deficient and -sufficient conditions. DNA Res. 2013; 20(2): 109-125.
31. Casas E, Cai G, Neill JD. Characterization of circulating transfer RNA-derived RNA fragments in cattle. Front Genet. 2015; 6: 271.
32. Fu Y, Lee I, Lee YS, Bao X. Small non-coding transfer RNA-derived RNA fragments (tRFs): Their biogenesis, function and implication in human diseases. Genomics Inform. 2015; 13(4): 94-101.
33. Anderson P, Ivanov P. tRNA fragments in human health and disease. FEBS Lett. 2014; 588: 4297-4304.
34. Karaiskos S, Grigoriev A. Dynamics of tRNA fragments and their targets in aging

mammalian brain. F1000Res. 2016; 5.
35. Kang L, Li S, Xing Z, Li J, Su Y, Fan P, et al. Dihydrotestosterone treatment delays the conversion from mild cognitive impairment to Alzheimer's disease in SAMP8 mice. Horm Behav. 2014; 65(5): 505-515.
36. Olvedy M, Scaravilli M, Hoogstrate Y, Visakorpi T, Jenster G, Martens-Uzunova ES. A comprehensive repertoire of tRNA-derived fragments in prostate cancer. Oncotarget. 2016; 7(17): 24766-24777.
37. Wei C, Salichos L, Wittgrove CM, Rokas A, Patton JG. Transcriptome-wide analysis of small RNA expression in early zebrafish development . RNA. 2012; 18(5): 915-929.
38. Karaiskos S, Naqvi AS, Swanson KE, Grigoriev A. Age-driven modulation of tRNA-derived fragments in Drosophila and their potential targets. Biol Direct. 2015; 10(1): 51.
39. Kumar P, Anaya J, Mudunuri SB, Dutta A. Meta-analysis of tRNA derived RNA fragments reveals that they are evolutionarily conserved and associate with AGO proteins to recognize specific RNA targets. BMC Biol. 2014; 12: 78.
40. Jovanovic K, Chetty CJ, Khumalo T, Da Costa Dias B, Ferreira E, Malindisa ST, et al. Novel patented therapeutic approaches targeting the 37/67 kDa laminin receptor for treatment of cancer and Alzheimer's disease. Expert Opin Ther Pat. 2015; 25(5): 567-582.
41. Humphries CE, Kohli MA, Nathanson L, Whitehead P, Beecham G, Martin E, et al. Integrated Whole Transcriptome and DNA Methylation Analysis Identifies Gene Networks Specific to Late-Onset Alzheimer's Disease. J Alzheimers Dis. 2015; 44(3): 977-987.
42. Li WX, Dai SX, Liu JQ, Wang Q, Li GH, Huang JF. Integrated Analysis of Alzheimer's Disease and Schizophrenia Dataset Revealed Different Expression Pattern in Learning and Memory. J Alzheimers Dis. 2016; 51(2): 417-425.
43. Martín-Maestro P, Gargini R, Perry G, Avila J, García-Escudero V. PARK2 enhancement is able to compensate mitophagy alterations found in sporadic Alzheimer's disease. Hum Mol Genet. 2015; 25(4): 792-806.
44. Delekate A, Füchtemeier M, Schumacher T, Ulbrich C, Foddis M, Petzold GC. Metabotropic P2Y1 receptor signalling mediates astrocytic hyperactivity in vivo in an Alzheimer’s disease mouse model. Nat Commun; 2014; 5: 5422.
45. Clark JD, Gebhart GF, Gonder JC, Keeling ME, Kohn DF. The 1996 guide for the care and use of laboratory animals. ILAR J. 1997; 38(1): 41-48.
46. Zhang S, Zhu DN, Li H, Zhang HJ, Feng CQ, Zhang WS. Analyses of mRNA profiling through RNA sequencing on a SAMP8 mouse model in response to ginsenoside Rg1 and Rb1 treatment. Front Pharmacol. 2017; 8: 88.
47. Martin M. Cutadapt removes adapter sequences from high-throughput sequencing reads. EMBnet J. 2011; 17(1): 10-12.
48. Chan PP, Lowe TM. GtRNAdb 2.0: an expanded database of transfer RNA genes identified in complete and draft genomes. Nucleic Acids Res. 2016; 44(D1): D184-D189.
49. Wang X, Zhu Y, Xu BO, Wang J, Liu X. Identification of TLR2 and TLR4-induced

microRNAs in human mesenchymal stem cells and their possible roles in regulating TLR signals. Mol Med Rep. 2016; 13(6): 4969-4980.
50. Jagadeeswaran G, Nimmakayala P, Zheng Y, Gowdu K, Reddy UK, Sunkar R. Characterization of the small RNA component of leaves and fruits from four different cucurbit species. BMC genomics. 2012; 13(1): 329.
51. Young MD, Wakefield MJ, Smyth GK, Oshlack A. Gene ontology analysis for RNA-seq: accounting for selection bias. Genome Biol. 2010; 11(2): R14.

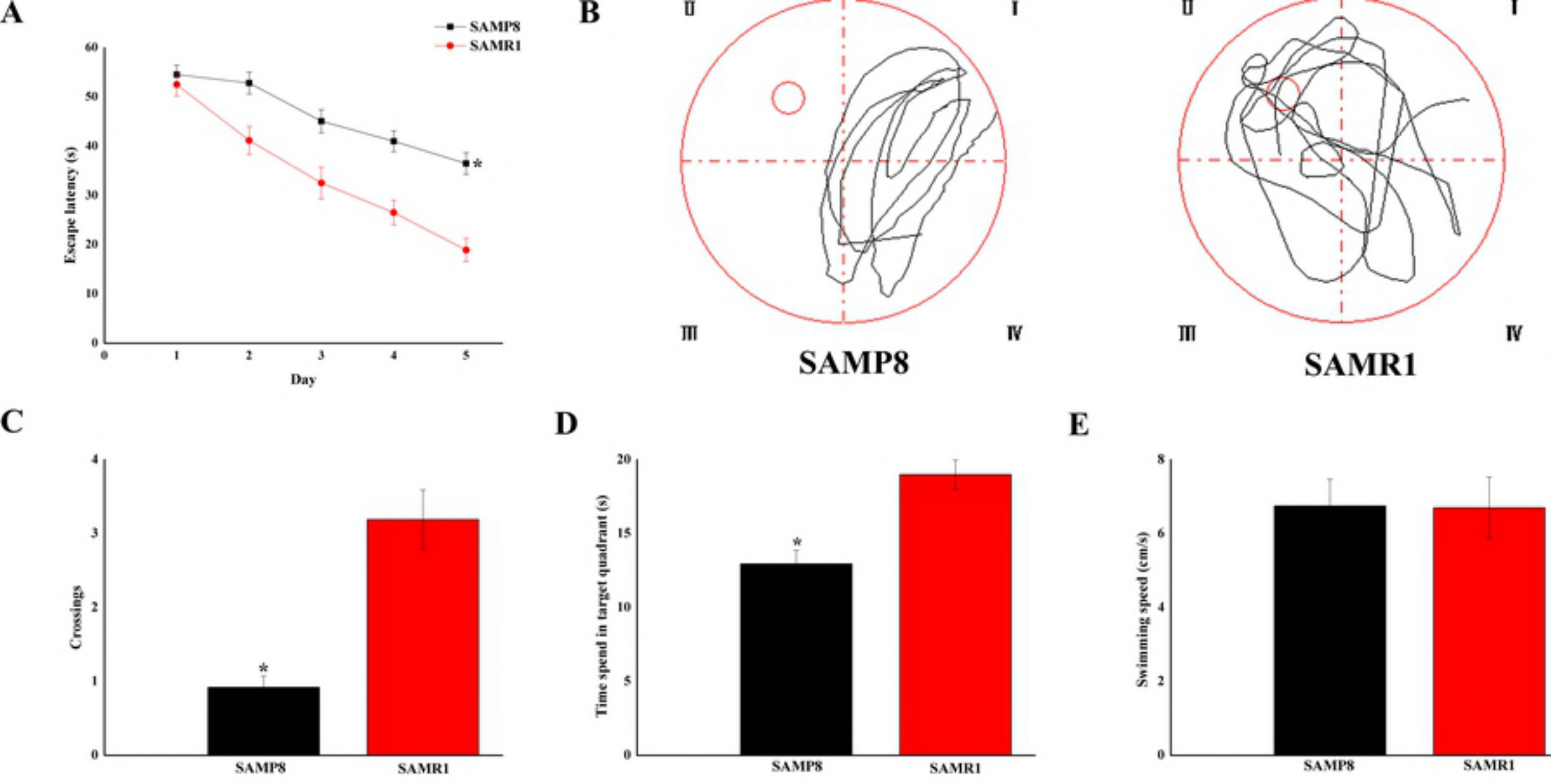
A
SAMP8
SAMR1
Escape latency (s)
Day
B
Ⅱ
Ⅰ
Ⅲ
Ⅳ
SAMP8
SAMR1
C
Crossings
SAMP8
SAMR1
D
Time spend in target quadrant (s)
SAMP8
SAMR1
E
Swimming speed (cm/s)
SAMP8
SAMR1

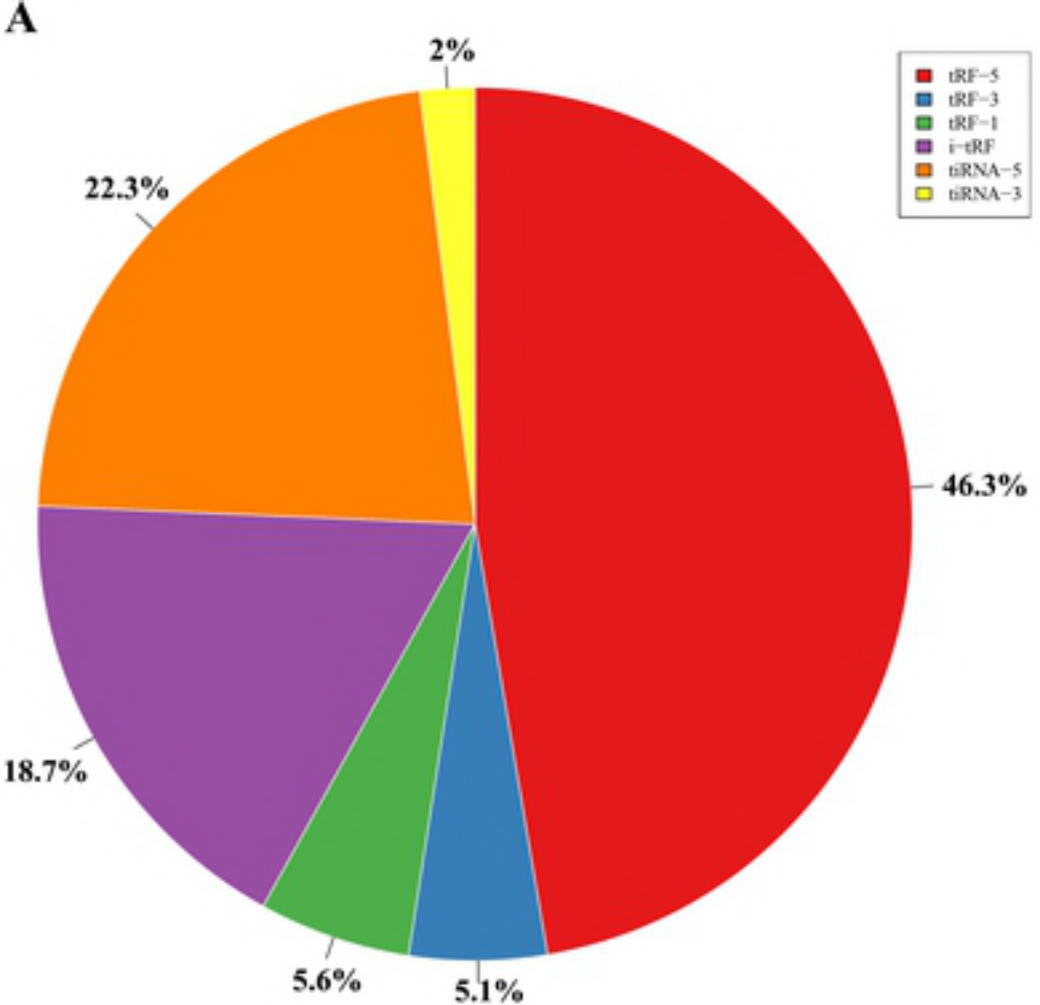
A
2%
22.3%
46.3%
18.7%
5.6%
5.1%
tRF−5
tRF−3
tRF−1
i−tRF
tiRNA−5
tiRNA−3

SAMP8

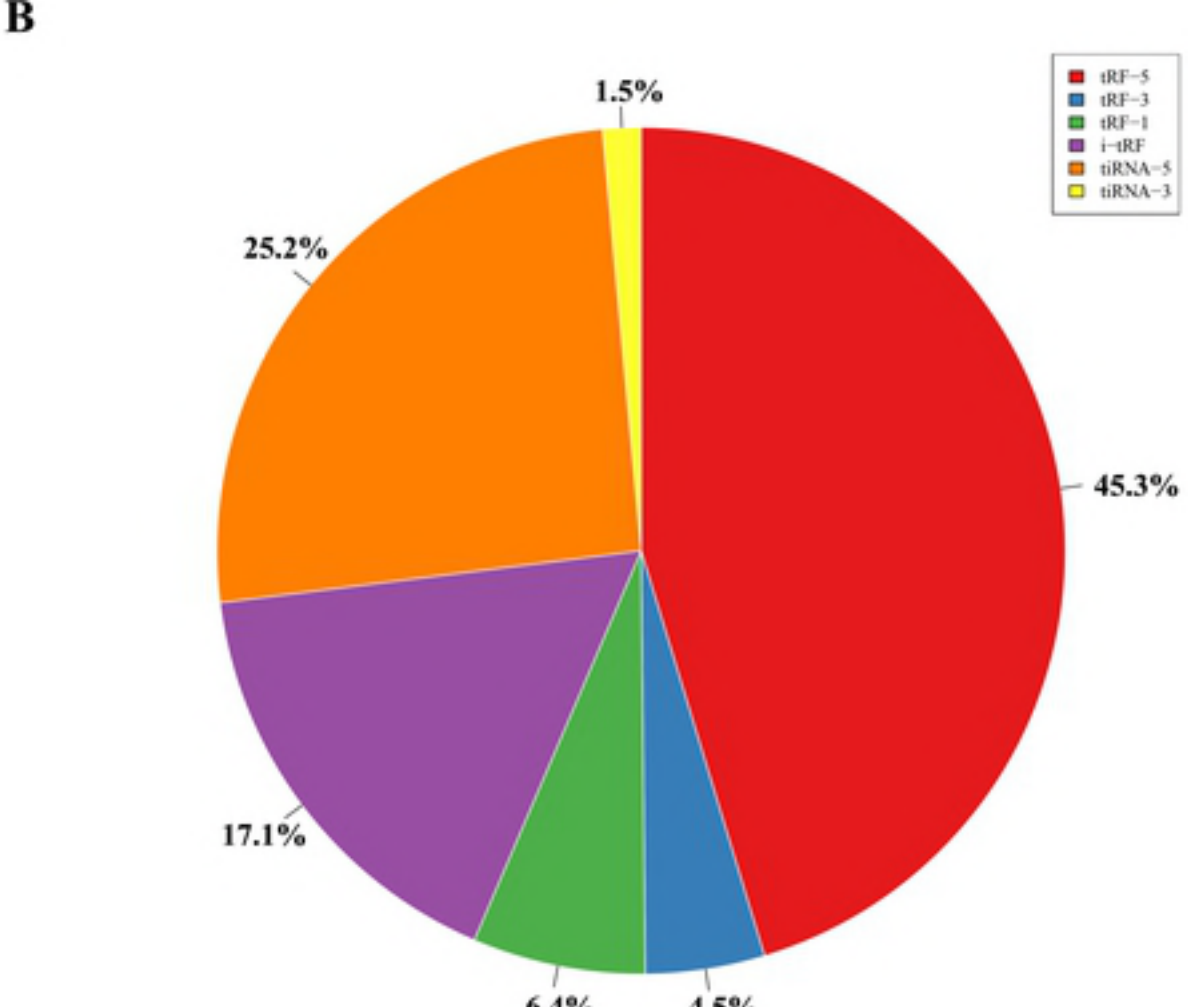
B
1.5%
25.2%
45.3%
17.1%
6.4%
4.5%
tRF−5
tRF−3
tRF−1
i−tRF
tiRNA−5
tiRNA−3

SAMR1

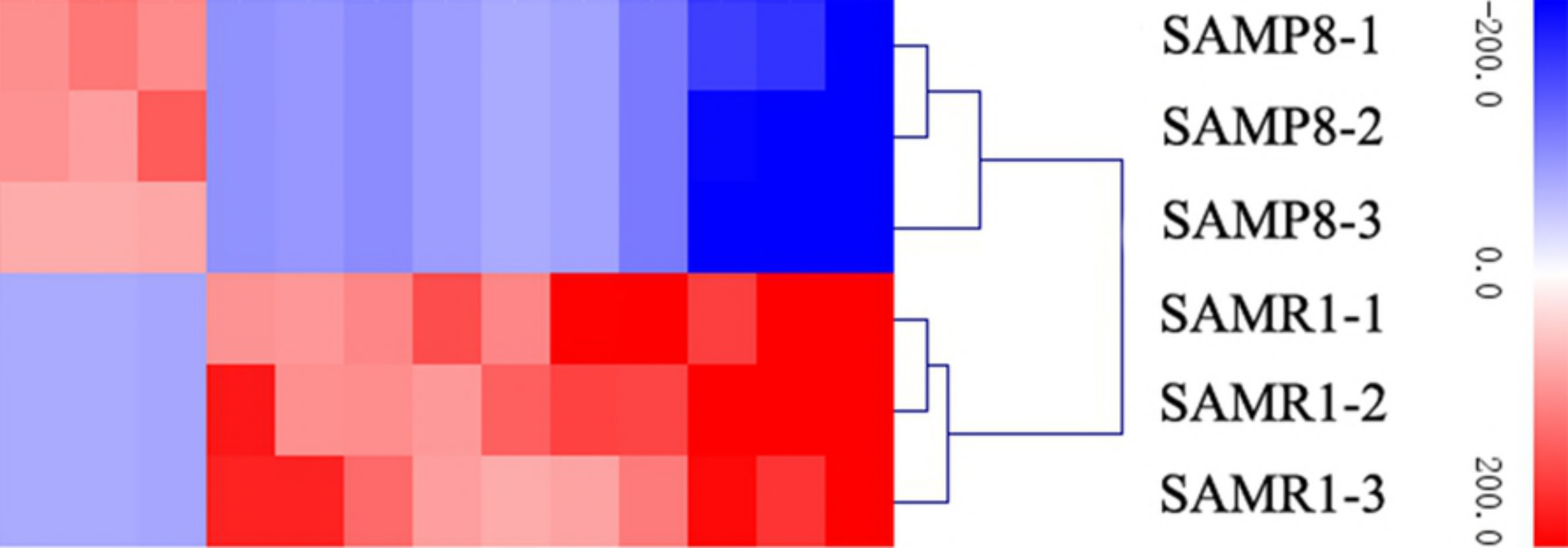
SAMP8-1
SAMP8-2
SAMP8-3
SAMR1-1
SAMR1-2
SAMR1-3
-200.0
0.0
200.0

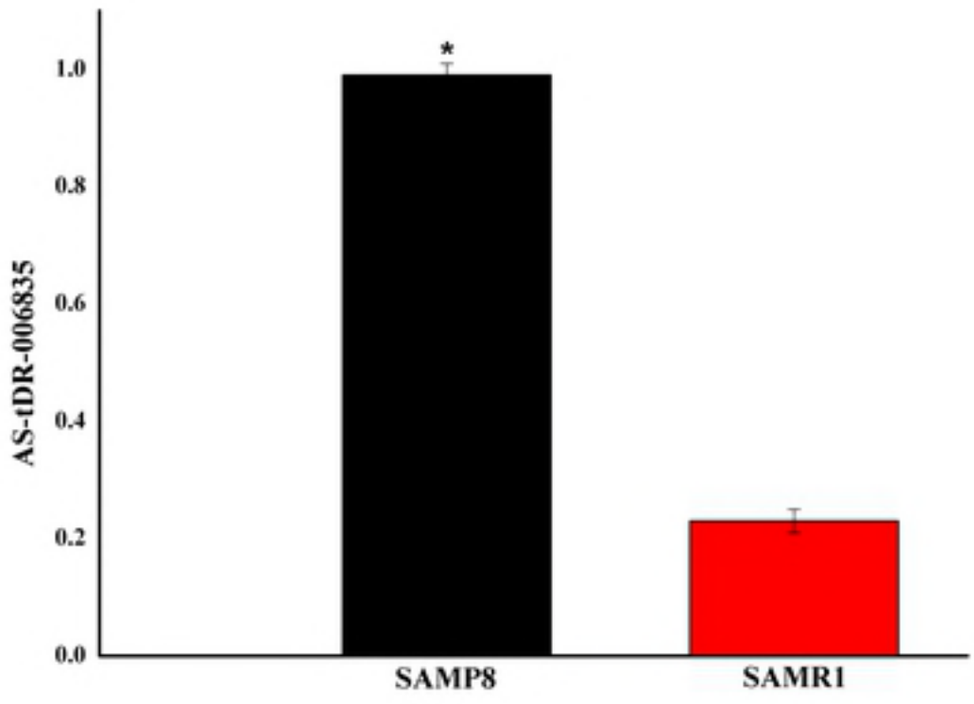
AS-tDR-006835
1.0
0.8
0.6
0.4
0.2
0.0
*
SAMP8
SAMR1

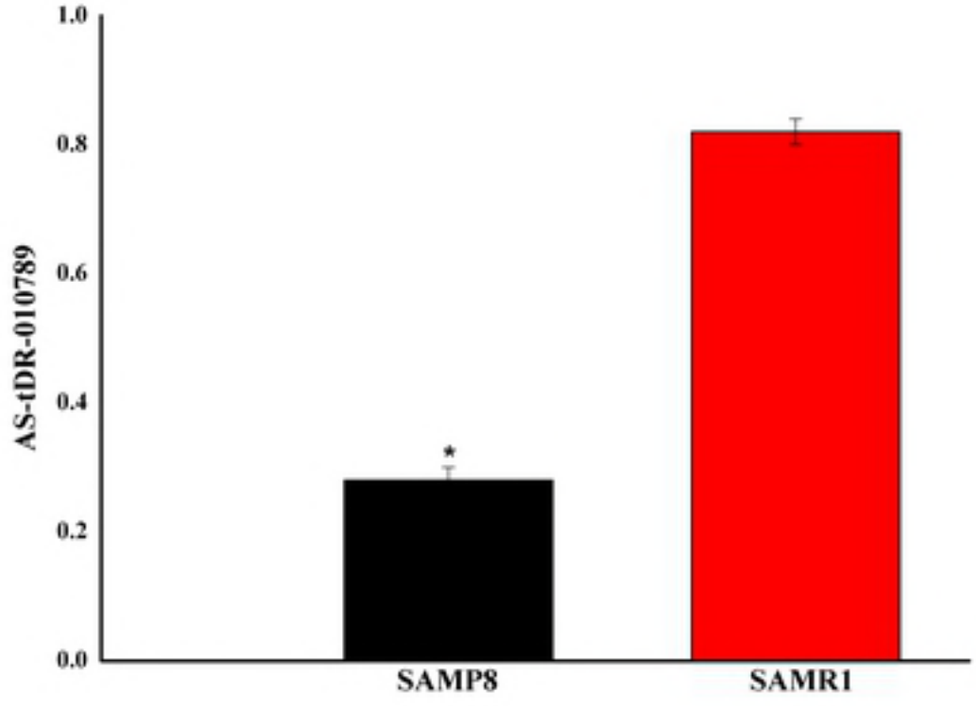
AS-tDR-010789
1.0
0.8
0.6
0.4
0.2
0.0
*
SAMP8
SAMR1

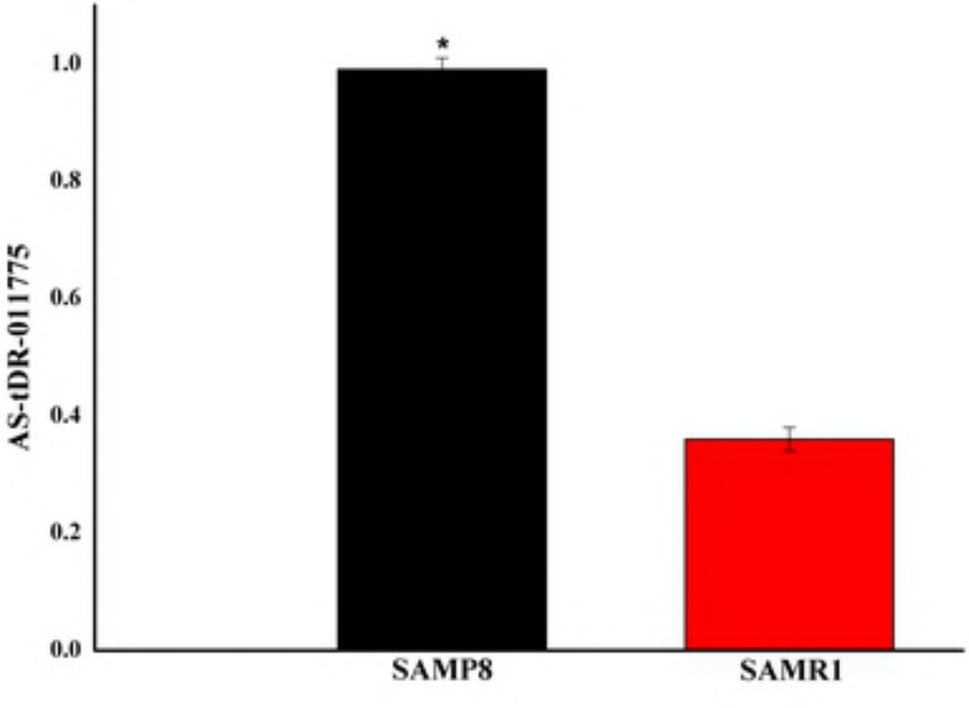
AS-tDR-011775
1.0
0.8
0.6
0.4
0.2
0.0
*
SAMP8
SAMR1

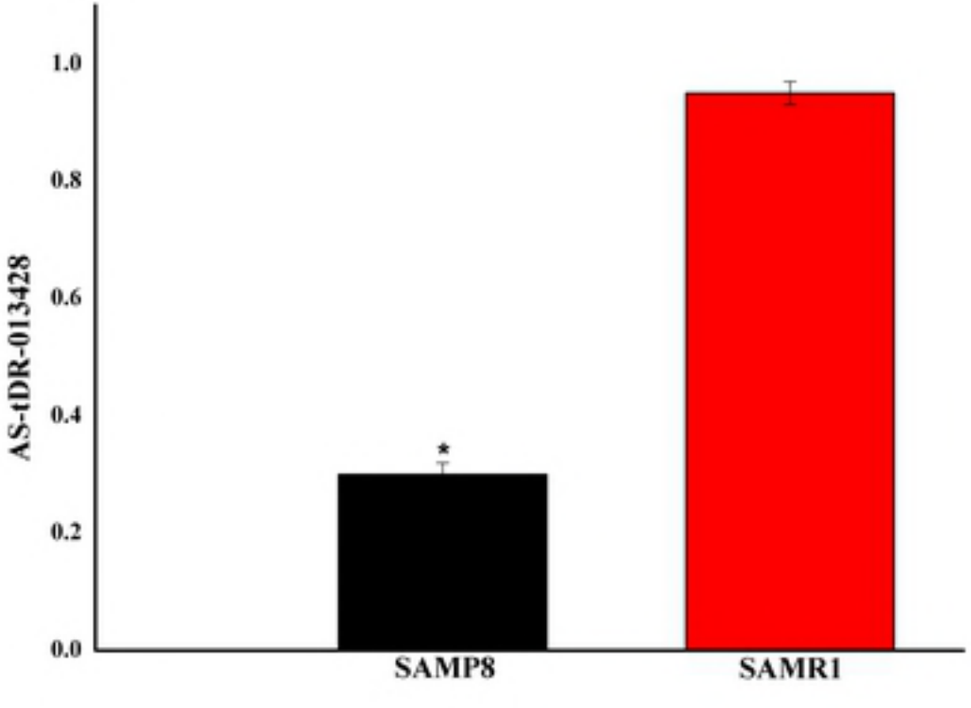
AS-tDR-013428
1.0
0.8
0.6
0.4
0.2
0.0
*
SAMP8
SAMR1